



DYNAMIC MODEL AND EARTHQUAKE RESPONSE OF A HYBRID ISOLATED SYSTEM WITH TUNED INERTER DAMPERS FOR NUCLEAR POWER PLANTS

Yixin Feng¹, Shaoping Li², Rong Pan³, Hao Xv⁴, Wenguang Liu⁵

¹ Ph. D., Shanghai Minhang Polytechnic, Shanghai, China

² Professor of engineering, Shanghai Nuclear Engineering Research & Design Institute, Shanghai, China

³ Professor, Ministry of Ecology and Environment of the People's Republic of China, Beijing, China

⁴ Research Associate Shanghai University, Shanghai, China

⁵ Professor, Shanghai University, Shanghai, China (13791980@qq.com), Corresponding author

ABSTRACT

Considering the benefits of tuned inerter damper (TID), a hybrid control system (TIDISO system) for third-generation NPPs consisting of an un-isolated outer containment structure, an isolated inner containment structure and a connecting TID system was proposed. First, governing equations of motion for the 3-degree-of-freedom (3DOF) model were derived and the seismic response variances of TIDISO system under white noise excitation were obtained. Next, an optimization study on inertance, frequency and damping parameters was conducted, and then simplified expressions were provided as a function of the various structural parameters for the optimal TID parameters. Finally, a case study was conducted to demonstrate the proposed rapid-determining formula for optimal TID parameters and to estimate the effectiveness of the proposed TIDISO system under seismic waves. The results illustrate the proposed system is effective to suppress acceleration and story drift responses, especially for isolation displacement. Under artificial wave 1, the displacement of isolation layer has declined from 436mm to 276mm, nearly 36%.

INTRODUCTION

Improving seismic performance is a key issue at the present because the high seismic objectives are required for NPP structures (Zhuang, 2017). Some previous studies have focused on the isolation technique in NPPs and excessive isolation displacement under strong earthquake may be one of the challenges. Wang et al. (2018) focused on the seismic response of base-isolated AP1000 nuclear shield building and the study found the displacements of the isolation layer exceed the maximum permissible deformation value of the isolation bearing. Similar conclusions that control seismic displacement of isolation layer is necessary are drawn by Huang et al. (2013), Zhu et al. (2017), Kumar S and Kumar M (2021). Some studies focused on increasing the damping of isolation layer to control displacement (Zhou Y. and Chen P., 2017) (Kelly JM, 1999). However, this will increase the equivalent dynamic stiffness and lead to the increase in acceleration. There are some studies on the strategy which is attaching tuned mass damper (TMD), inertial dampers to the isolated structure (Taniguchi T., et. al, 2008) (Takewaki I., et al, 2012). It is significant to study the hybrid isolated control strategies, to control seismic response for important buildings, especially for NPPs.

The tuned inerter damper (TID) has been proposed by Lazar IF et al (2014) at first. However, the TID can easily provide a large inertance with incredibly small physical mass and a large damping force can be provided. That means the TID is not only used as resonant-type damper but also viscous damper. The correlational research has exhibited an explosively increasing trend in civil engineering over the past decade. Gonzalez-Buelga A. et al (2017) conducted the experimental analysis on TID to verify its performance as a vibration absorber. The optimization study on high-rise buildings using TID has been conducted by Daniel Caicedo et al. (2021). In paper by Xu et al. (2021) a closed-form formula for optimal

TID parameters based on equivalent linearization method is derived. Considering this advantageous feature of inerter, some hybrid control systems consisted of isolation and TID was proposed to enhance the effectiveness of isolation technique. An optimization study on H-2 norm performances of TID-isolated system was conducted using a two-degree-of-freedom model (2DOF) and closed-form solutions for key parameters were provided in paper by Sun et al (2021). Excessive displacements of the isolated structure could be eliminated by supplementing a TID were obtained by Patrice Nyangi and Ye Kun (2021). Hence, hybrid isolated control systems with TID may be worth investigating.

The third-generation NPP generally adopts double reactor containment structure to comprehensively improve security, such as the Hua-long Pressurized Reactor (HPR1000) and European Pressurized Reactor (EPR) (Czech J., 1999). It is similar to the adjacent structures in civil engineering. In terms of adjacent structures, the benefits of connected control method (CCM) have been proved by many researchers (Christenson Richard E., 2007, Palermo M., 2020). In this paper, a hybrid control system for the third-generation NPPs named as TIDISO system which consists of a flexible outer containment structure, an isolated inner containment structure and tuned inerter damper (TID) system was proposed to control the vibration shown in Figure 1.

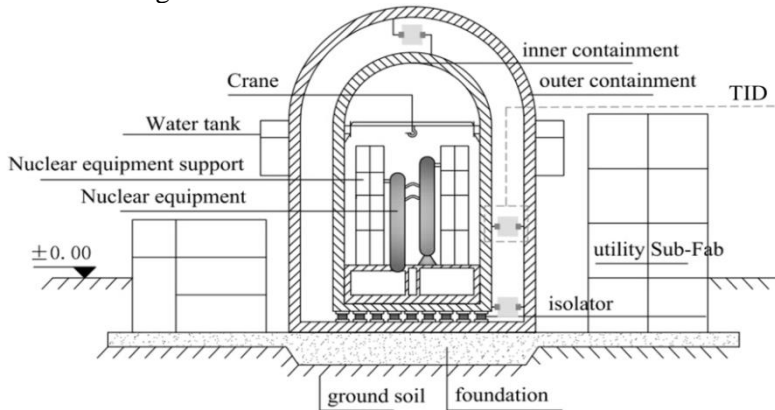


Figure 1. Concept of TIDISO control system

THEORETICAL MODEL OF TIDISO HYBRID CONTROL SYSTEM

Governing equations of motion

The TIDISO system can be simplified as a 3-degree of freedom model (hereinafter to be referred as 3-DOF model) shown in Figure 2. The outer containment structure is un-isolated and reduced as a lumped mass model (hereinafter to be referred as outer structure), where m_o , k_o and c_o denote mass, stiffness and damping coefficient respectively. The inner containment structure and the equipment are isolated and reduced as a lumped mass model (hereinafter to be referred as inner structure). The m_i , k_i and c_i denote the mass, stiffness and damping coefficient. k_i is the equivalent stiffness of the isolators. c_i is the equivalent damping coefficient of the isolators. b , c and k are the inertance of the TID, the damping coefficient of the TID and the stiffness of the TID.

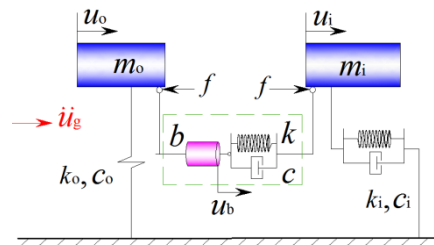


Figure 2. 3DOF model of TIDISO control system for NPPs with double containments

The equations of motion can be written in the uniform matrix form as Equation (1).

$$\mathbf{M}\{\ddot{u}\} + \mathbf{C}\{\dot{u}\} + \mathbf{K}\{u\} = -\mathbf{ME}\{\ddot{u}_g\} \quad (1)$$

Where, M, C and K are the mass, damping and stiffness matrices of the TIDISO systems. $\mathbf{E}=[1 \ 1 \ 1]^T$ is the influence vector. $\{\ddot{u}\}$, $\{\dot{u}\}$ and $\{u\}$ are the acceleration, velocity and displacement vector, respectively.

$$\mathbf{M} = \begin{bmatrix} m_o + b & -b \\ -b & m_i & b \\ -b & b & b \end{bmatrix}, \quad \mathbf{C} = \begin{bmatrix} c_o & & \\ & c_i & \\ & -c & c \end{bmatrix}, \quad \mathbf{K} = \begin{bmatrix} k_o & & \\ & k_i & \\ & -k & k \end{bmatrix}, \quad \{\ddot{u}\} = \begin{bmatrix} \ddot{u}_o \\ \ddot{u}_i \\ \ddot{u}_b \end{bmatrix}, \quad \{\dot{u}\} = \begin{bmatrix} \dot{u}_o \\ \dot{u}_i \\ \dot{u}_b \end{bmatrix}, \quad \{u\} = \begin{bmatrix} u_o \\ u_i \\ u_b \end{bmatrix}$$

Defined the state vector of TIDISO system as Equation (2)

$$\mathbf{Y} = [u_o \ u_i \ u_b \ \dot{u}_o \ \dot{u}_i \ \dot{u}_b]^T, \quad \dot{\mathbf{Y}} = [\dot{u}_o \ \dot{u}_i \ \dot{u}_b \ \ddot{u}_o \ \ddot{u}_i \ \ddot{u}_b]^T \quad (2)$$

The related state-space equations can be written as Equation (3)

$$\dot{\mathbf{Y}}_{(6^*1)} = \mathbf{AY}_{(6^*1)} + \mathbf{Bu} \quad (3)$$

Where, $\mathbf{A} = \begin{bmatrix} \mathbf{0}_{(3^*3)} & \mathbf{I}_{(3^*3)} \\ -\mathbf{M}^{-1}\mathbf{K} & -\mathbf{M}^{-1}\mathbf{C} \end{bmatrix}$, $\mathbf{B} = \begin{bmatrix} \mathbf{0}_{(3^*1)} \\ -\mathbf{M}^{-1}\mathbf{ME} \end{bmatrix}$, $\mathbf{u} = \ddot{u}_g$. $\mathbf{0}_{3^*3}$ and \mathbf{I}_{3^*3} represent the 3^*3 zero matrix and identity matrix, respectively.

The output equation is set as Equation (4)

$$\mathbf{Z} = \mathbf{CY} + \mathbf{Du} \quad (4)$$

Where, the outputs include relative displacement and absolute acceleration of the outer and inner structures, as well as relative displacement and absolute acceleration of TID. $\mathbf{D} = 0$

$$\mathbf{Z} = [u_o \ u_i \ u_b \ \ddot{u}_o + \ddot{u}_g \ \ddot{u}_i + \ddot{u}_g \ \ddot{u}_b + \ddot{u}_g]^T, \quad \mathbf{C} = \begin{bmatrix} \mathbf{0}_{(3^*3)} & \mathbf{0}_{(3^*3)} \\ \mathbf{0}_{(3^*3)} & \mathbf{E}_{(3^*3)} \end{bmatrix} \left[\begin{bmatrix} \mathbf{0}_{(3^*3)} & \mathbf{I}_{(3^*3)} \\ -\mathbf{M}^{-1}\mathbf{K} & -\mathbf{M}^{-1}\mathbf{C} \end{bmatrix} + \begin{bmatrix} \mathbf{E}_{(3^*3)} & \mathbf{0}_{(3^*3)} \\ \mathbf{0}_{(3^*3)} & \mathbf{0}_{(3^*3)} \end{bmatrix} \right]$$

The transfer functions in the frequency domain between the ground motion acceleration and outputs including the respective relative displacement and absolute acceleration of the TIDISO system can be obtained as Equation (5)

$$H(s)_{(6^*1)} = \frac{\mathbf{Z}(s)}{\mathbf{u}(s)} = \frac{\mathbf{C}[s\mathbf{I} - \mathbf{A}]^{-1} \mathbf{Bu}(s)}{\mathbf{u}(s)} = \mathbf{C}_{(6^*6)} \left[s\mathbf{I}_{(6^*6)} - \mathbf{A}_{(6^*6)} \right]^{-1} \mathbf{B}_{(6^*1)} \quad (5)$$

The response variances of the relative displacement and absolute acceleration of TIDISO system can be calculated by Equation (6)

$$E[\dot{u}_j^2(t)] = (\|H_j(i\omega)\|_2)^2, \quad E[u_j^2(t)] = (\|H_j(i\omega)\|_2)^2, \quad (j=i, o) \quad (6)$$

PARAMETER STUDY

Parameter Correlation

The following new variables were introduced. ω_i , ω_o and ω_b are circular frequency of the inner structure, the outer structure and the TID system, respectively. ξ_o and ξ_i are damping ratio of the outer structure and inner structure, respectively. The mass ratio of the outer structure to the inner structure denotes μ_o . μ_b is the ratio of inertance of the TID to the mass of inner structure. The circular frequency ratio of the outer structure to the inner structure is α_o . The circular frequency ratio of TID to the inner structure is γ . κ is the damping coefficient ratio of TID to the inner structure.

$$\omega_i = \sqrt{\frac{k_i}{m_i}}, \quad \omega_o = \sqrt{\frac{k_o}{m_o}}, \quad \omega_b = \sqrt{\frac{k}{b}}, \quad \xi_i = \frac{c_i}{2\omega_i m_i}, \quad \xi_o = \frac{c_o}{2\omega_o m_o}, \quad \mu_o = \frac{m_o}{m_i}, \quad \mu_b = \frac{b}{m_i}, \quad \alpha_o = \frac{\omega_o}{\omega_i}, \quad \gamma = \frac{\omega_b}{\omega_i}, \quad \kappa = \frac{c}{c_i}$$

The non-dimensional structural variances of displacements and accelerations for TIDISO system are defined as Equation (7)

$$\beta_{-a_o} = \frac{E[\ddot{u}_o^2(t)]}{E_{uc}[\ddot{u}_o^2(t)]}, \quad \beta_{-a_i} = \frac{E[\ddot{u}_i^2(t)]}{E_{uc}[\ddot{u}_i^2(t)]}, \quad \beta_{-d_o} = \frac{E[u_o^2(t)]}{E_{uc}[u_o^2(t)]}, \quad \beta_{-d_i} = \frac{E[u_i^2(t)]}{E_{uc}[u_i^2(t)]} \quad (7)$$

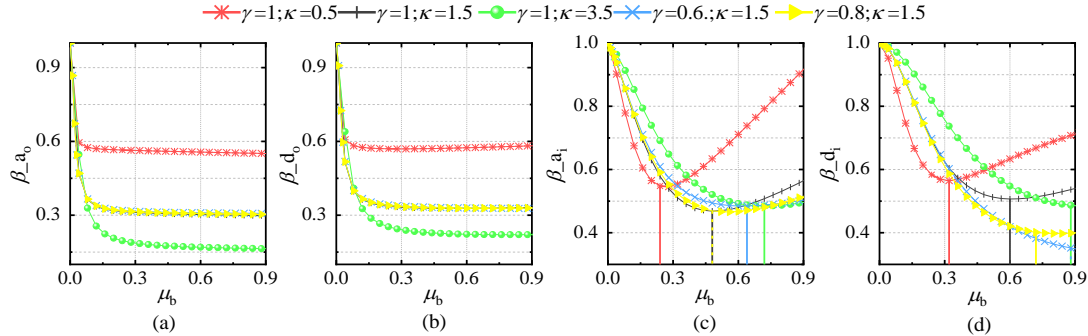


Figure 3 Nondimensional structural variances varying with μ_b with different parameters γ and κ [(a) acceleration of outer structure; (b) displacement of outer structure; (c) acceleration of inner structure (d) displacement of inner structure]

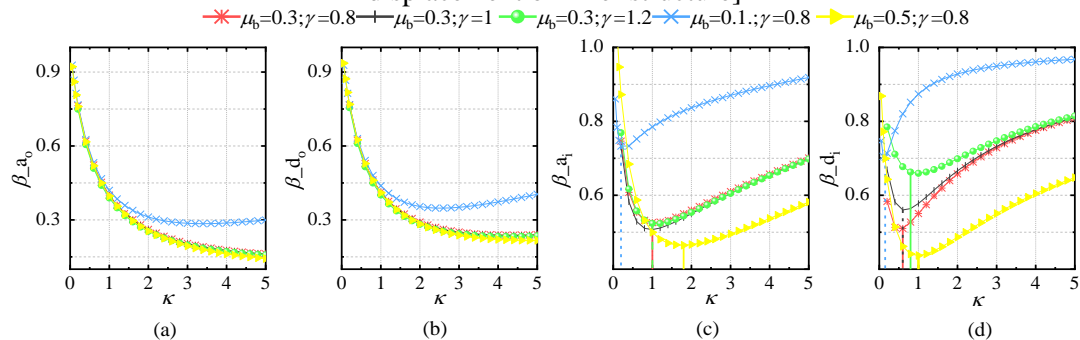


Figure 4 Nondimensional structural variances varying with κ with different parameters γ and μ_b [(a) acceleration of outer structure; (b) displacement of outer structure; (c) acceleration of inner structure; (d) displacement of inner structure]

To discuss the influence of TID parameters, including parameter μ_b , γ and κ , on system response, simulations are firstly conducted on the systems with the structural parameters: $\mu_o=0.4$, $\alpha_o=10$, $\xi_o=0.02$, $\xi_i=0.1$. In Figure 3 the influence of different parameter γ and parameter κ on the variation trends of displacement and acceleration response variances to parameter μ_b of the TID was reported. The results of correlation analysis are shown in Figure 4 for the parameter κ . Correlation analysis results are shown in

Figure 5. TIDISO system achieves better control performances for the un-isolated structure than those for isolated structure and the isolated structure is more sensitive to TID parameters.

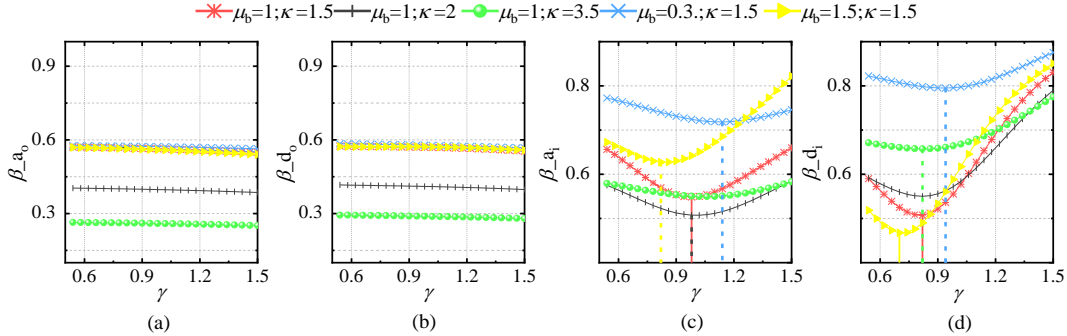


Figure 5 Nondimensional structural variances varying with γ with different parameters μ_b and κ [(a) acceleration of outer structure; (b) displacement of outer structure; (c) acceleration of inner structure; (d) displacement of inner structure]

H₂ optimal analysis

An objective function is defined as minimizing the mean value of non-dimensional acceleration and displacement variances of the inner structure shown as Equation (8) to conduct an optimization study. This minimization of this objective function leads to the optimal parameters including κ_{opt} and γ_{opt} of the TIDISO structure system.

$$Z = \frac{1}{2} \beta_{-} \ddot{u}_i + \frac{1}{2} \beta_{-} u_i \quad (8)$$

MATLALB software and a gradient-based searching technique were used to determine the optimal damping parameter κ_{opt} and frequency parameter γ_{opt} corresponding to different inertance parameter μ_b on the systems with the structural parameters: $\mu_0=0.4$, $\alpha_0=10$, $\xi_0=0.02$, $\xi_i=0.1$. Figure 6 presents the variation of objective Z with the damping parameter κ and the frequency parameter γ to the inner structure with different inertance parameter μ_b . Figure 7 presents the objective Z and optimal TID parameters κ_{opt} and γ_{opt} for the TIDISO systems under a set of certain structural parameter.

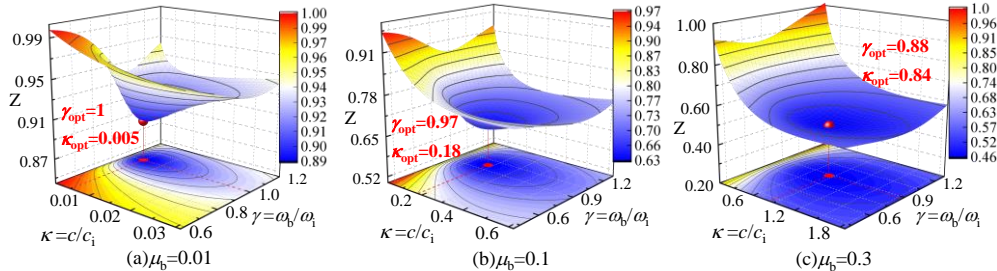


Figure 6 The variation of objective Z with κ and γ corresponding to different inertance parameter μ_b of 0.01, 0.1 and 0.9

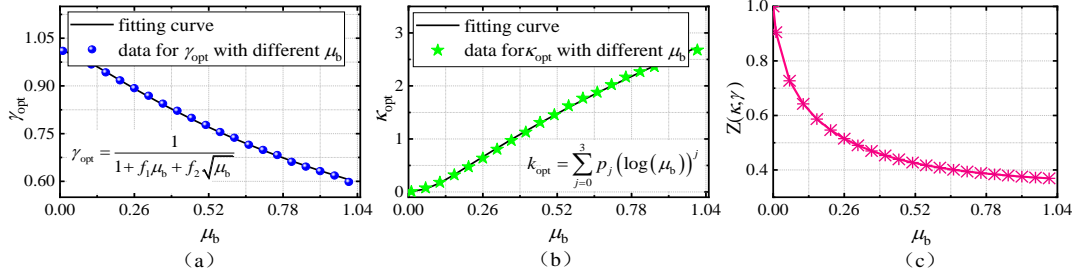


Figure 7 Optimal TID parameters κ_{opt} , γ_{opt} and objective Z corresponding to different inertance parameter μ_b

The curve fitting method was conducted to obtain the explicit expressions of optimal damping parameter κ_{opt} and the optimal frequency parameter γ_{opt} based on the massive numerical searching data of TID parameters. The Equation (9)(a)(b) were obtained respectively for the parameter γ_{opt} and κ_{opt} after several trials and errors.

$$\gamma_{\text{opt}} = \frac{1}{1 + f_1\mu_b + f_2\sqrt{\mu_b}} \quad (9)(a)$$

$$k_{\text{opt}} = p_0 + p_1 \log(\mu_b) + p_2 (\log(\mu_b))^2 + p_3 (\log(\mu_b))^3 \quad (9)(b)$$

Explicit expressions of TID parameters about various structural parameters

A curve fitting method is used to provide simplified expressions as a function of the various structural parameters for the choice of the optimal TID parameters. Structural parameters and TID parameters as well as their respective incremental intervals are shown in Table 1.

Table 1: Tables should be centred and preceded by a numbered caption

Parameter	Range	Step	Parameter	Range	Step
ξ_i	0.08-0.2	0.01	μ_b	0.01-1	0.05
α_o	3-23	2	κ	0.001-5	0.01
μ_o	0.1-0.9	0.05	γ	1.1-0.4	0.001

The expression of optimal frequency parameter γ_{opt} as a function of the various structural parameters was provided as Equation (10) and the coefficients are shown in Table 2. The expression of optimal damping parameter κ_{opt} as a function of the various structural parameters was provided as Equation (11) and the coefficients are shown in Table 3.

$$\gamma_{\text{opt}} = \frac{1}{1 + \left(2.92\xi_i + fff_{13} \left(\frac{1}{\alpha_o} \right)^2 + fff_{12} \frac{1}{\alpha_o} + fff_{11} \right) \mu_b + \left(-1.71\xi_i + fff_{23} \left(\frac{1}{\alpha_o} \right)^2 + fff_{22} \frac{1}{\alpha_o} + fff_{21} \right) \sqrt{\mu_b}} \quad (10)$$

Table 2: Coefficients of γ_{opt} fitting formula

fff11	fff12	fff13	fff21	fff22	fff23
0.538	-0.214	5.362	-0.013	0.097	-2.906

$$k_{\text{opt}} = \sum_{j=0}^3 \left(ppp_{j2} \xi_i^2 + \left(\sum_{t=0}^2 ppp_{jt} (\sqrt{\mu_o})^t \right) \xi_i + \left(\sum_{t=0}^2 ppp_{j0t} (\sqrt{\mu_o})^t \right) \right) (\log(\mu_b))^j \quad (11)$$

Table 3: Coefficient of κ_{opt} fitting formula

ppp_{000}	ppp_{001}	ppp_{002}	ppp_{010}	ppp_{011}	ppp_{012}	ppp_{100}	ppp_{101}	ppp_{102}
7.02	-1.87	0.56	-44.24	5.32	-1.74	15.41	-5.18	1.18
ppp_{110}	ppp_{111}	ppp_{112}	ppp_{200}	ppp_{201}	ppp_{202}	ppp_{210}	ppp_{211}	ppp_{212}
-101.07	17.6	-4.55	11.35	-4.46	0.76	-77.38	16.93	-3.64
ppp_{300}	ppp_{301}	ppp_{302}	ppp_{310}	ppp_{311}	ppp_{312}			
2.61	-1.17	0.16	-17.68	4.73	-0.9			

ESTIMATING THE PERFORMANCE OF TIDISO SYSTEM UNDER SEISMIC WAVES

Analysis model and Seismic Waves

The structural MDOF model introduced in

Table 4 which has been used in previous study (Djerouni S, 2021) was adopted to carry out time history analyses. The initial stiffness of isolation layer is about $12.3e7$ N/m, the post-yield stiffness is $0.949e7$ N/m. Yield force is 300480N and the ratio of yield force to weight is nearly 2%. The yield coefficient, the ratio of post-yield stiffness to initial stiffness, is about 0.076. Both of the damping ratios of superstructure for building “o” and building “i” are 2%.

Table 4: Model information of structural MDOF

	multi-degree-of-freedom model			3-degree-of-freedom model			Damping Coeficient (10^5 N*s/m)
	node No.	mass (10^4 Kg)	Stiffness (10^7 N/m)	node No.	mass (10^4 Kg)	Stiffness (10^7 N/m)	
Buildin g “o”	1	21.52	14.7	“o”	89.75	5.45	2.8
	2	20.92	11.3				
	3	20.7	9.9				
	4	26.61	8.4				
Buildin g “i”	5 (Isolation layer)	40	12.3/0.949	“i”	150.23	0.98	6.5
	6	21.52	14.7				
	7	20.92	11.3				
	8	20.7	9.9				
	9	20.48	8.9				
	10	26.61	8.4				

Three earthquake ground motions were considered for the present study. All the time step of the three seismic waves is 0.005s. In order to keep the comparisons between different records at the same level, all the peak acceleration of these natural earthquake records was scaled to 0.6 g. The time histories and are shown in Figure 8.

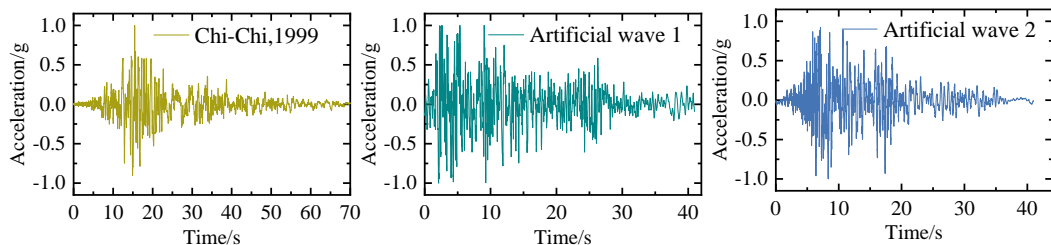


Figure 8 Time histories of 3 ground motions

Seismic response of TIDISO system

The MDOF structural model was reduced to the corresponding equivalent 3DOF model to utilize the proposed expressions of optimal TID parameters. More details are shown as Table 4. The cases of the numerical analysis are shown as Table 5.

Table 5: Cases of the numerical analysis for TIDISO control system

Case No.	μ_b	K_{opt}	γ_{opt}	connected node No.	Ground motion
1	0.2	0.5423	0.938	4-9	Chi-Chi,1999
2	0.2	0.5423	0.938	4-9	Artificial wave 1
3	0.2	0.5423	0.938	4-9	Artificial wave 2
4	0.2	0.5423	0.938	2-7	Chi-Chi,1999
5	0.2	0.5423	0.938	2-7	Artificial wave 1
6	0.2	0.5423	0.938	2-7	Artificial wave 2
7	0.2	0.5423	0.938	1-5	Chi-Chi,1999
8	0.2	0.5423	0.938	1-5	Artificial wave 1
9	0.2	0.5423	0.938	1-5	Artificial wave 2

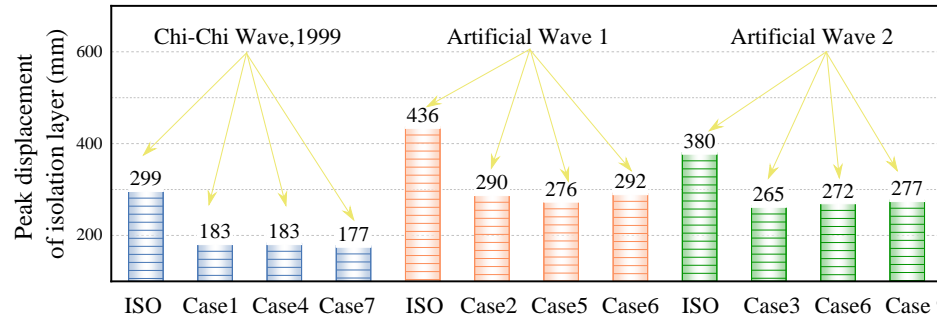


Figure 9 Comparison of peak isolation layer displacement between ISO system and TIDISO system

The peak isolation layer displacement decreases substantially shown as Figure 9. The placement of TID has low impact on the isolation layer displacement. J_d and J_a are defined as Equation (12), corresponding to story drift and acceleration are normalized by those of ISO system only.

$$J_a = \text{rms}(a_j) / \text{rms}(a_j^{uc}), \quad J_d = \text{rms}(d_j) / \text{rms}(d_j^{uc}) \quad (12)$$

Where, j is the node number.

Figure 10 shows the comparison results of the RMS values of absolute accelerations and the story drifts among uncontrolled structural system (without any control devices and hereinafter referred to as UC system), ISO (the inner structure is isolated) and TIDISO system under Chi-Chi wave. All TIDISO cases perform better than the ISO case in terms of reducing the seismic suppression ratio J_a from Figure 10 (a). The higher placement of the TID leads better seismic suppression performance and the seismic suppression ratio of the top floor acceleration is about 0.8 under the best case for the outer structure. Similar results for seismic suppression ratio J_d can be observed in Figure 10 (b). For the floor which is connected to the TID, its story drift is not reduced even slightly increased because the damping force is concentrated.

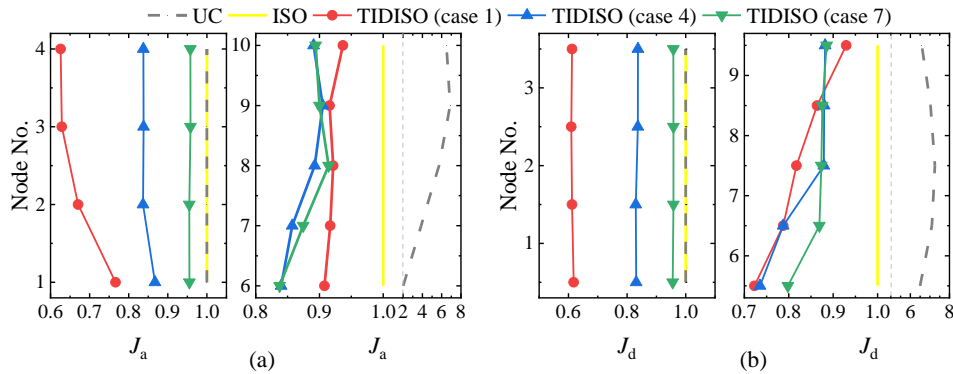


Figure 10 Normalized root mean square (RMS) acceleration and displacement response under Chi-Chi wave

CONCLUSION

The governing equations of motion for 3DOF simplified model were derived and the seismic response variances of TIDISO system under white noise excitation were obtained. An optimization study was conducted to determine the optimal damping parameter κ_{opt} and frequency parameter γ_{opt} of the TID, whereby the mean value of non-dimensional acceleration and displacement variances of the isolated structure is adopted as an objective function based on the results of parameter correlation analysis. In addition, simplified expressions were provided as a function of the various structural parameters for the optimal TID parameters. A case study was conducted to demonstrate the proposed rapid-determining expressions and estimate the effectiveness of the proposed system under seismic waves. The principal outcomes of this research are summarized as follows:

(1) For TIDISO system, higher TID inertance can improve more seismic suppression effectiveness due to its greater damping force. The rate of the objective Z decreases slower with the increase of parameter μ_b .

(2) The simplified expressions of optimal TID parameters were obtained by using the curve fitting method. The optimal TID damping parameter and frequency parameter can be obtained according to structural parameters and it is easy to use to engineering applications.

(3) According to the results of case study, the displacement of the isolation layer was effectively controlled without any increases in other indicators including acceleration and the story drift. In the best case, the displacement decreased from 436mm to 276mm, nearly 36%.

It is noted that how to improve the accuracy of fitting formula should be considered in further studies. And the optimization research on the layout of TID should be conducted for guiding engineering designs.

REFERENCES

- Zhuang C. L., Zhang Y. S., Wang D. Y. (2017). "Effects of seismic action and material properties variations on seismic responses of base-isolated nuclear containment structure," *Annals of Nuclear Energy*, UK, 110(dec.): 909-919.
- Wang D., Zhuang C., Zhang Y. (2018). "Seismic response characteristics of base-isolated AP1000 nuclear shield building subjected to beyond-design basis earthquake shaking," *Nuclear Engineering and Technology*, NL, 50:170-181.
- Huang Y. N., Whittaker A. S., Kennedy R. P. (2013). "Response of Base-Isolated Nuclear Structures for Design and Beyond-Design Basis Earthquake Shaking," *Earthquake Engineering and Structural Dynamics*, USA, 42: 339-356.

- Zhu X.Y., Lin G., Pan R. (2017). "Influence Analysis on Seismic Response of Reactor Building of NPP Affected by Base-seismic Isolation," *Atomic Energy Science and Technology*, CHN, 51(4): 706-712. (in Chines)
- Kumar S., Kumar M. (2021). "Damping implementation issues for in-structure response estimation of seismically isolated nuclear structures," *Earthquake Engineering and Structural Dynamics*, USA, 50: 1967-1988.
- Zhou Y., Chen P. (2017). "Shaking table tests and numerical studies on the effect of viscous dampers on an isolated RC building by friction pendulum bearings," *Soil Dynamics and Earthquake Engineering*, UK, 100:330-344.
- Kelly JM. (1999). "The role of damping in seismic isolation," *Earthquake Engineering and Structural Dynamics*. USA, 28:3-20.
- Taniguchi T., Kiureghian A. D., Melkumyan M. (2008). "Effect of tuned mass damper on displacement demand of base-isolated structures," *Engineering Structures*, UK, 30(12):3478-3488.
- Takewaki I., Murakami S., Yoshitomi S. (2012). "Fundamental mechanism of earthquake response reduction in building structures with inertial dampers," *Structural Control and Health Monitoring*, UK, 19(6): 590-608.
- Lazar I. F., Neild S. A., Wagg D. J. (2014). "Using an inerter-based device for structural vibration suppression," *Earthquake Engineering and Structural Dynamics*, USA, 43(8):1129-1147.
- Gonzalez-Buelga A , Lazar I F , Jiang J Z , et al (2017). "Assessing the effect of nonlinearities on the performance of a tuned inerter damper," *Structural Control and Health Monitoring*, UK, 24(3).
- Caicedo D , Lara L A , Blandon J , et al (2021). "Seismic response of high-rise buildings through metaheuristic-based optimization using tuned mass dampers and tuned mass dampers inerter," *Journal of Building Engineering*, NLD, 34(1):20
- Xu T , Li Y , Lai T , et al (2021). "A simplified design method of tuned inerter damper for damped civil structures: Theory, validation, and application," *Structural Control and Health Monitoring*, UK 28(9)
- Sun H., Zuo L., Wang X., et al. (2019). "Exact H2 optimal solutions to inerter-based isolation systems for building structures," *Structural Control and Health Monitoring*, UK, 26(6).
- Angelis M D , Giaralis A , Petrini F , et al. (2019) "Optimal tuning and assessment of inertial dampers with grounded inerter for vibration control of seismically excited base-isolated systems," *Engineering Structures*, UK, 196(OCT.1):109250.1-109250.19.
- Nyangi Patrice, Ye Kun (2021). "Optimal design of dual isolated structure with supplemental tuned inerter damper based on performance requirements," *Soil Dynamics and Earthquake Engineering*, UK, 149,106830.
- Czec h J., Wirkner J., Yvon M., et al (1999). "European pressurized water reactor: safety objectives and principles," *Nuclear Engineering and Design*, USA, 187(1):25-32.
- Christenson Richard E., Spencer. Billie F., Johnson Erik A. (2007). "Semiactive connected control method for adjacent multidegree-of-freedom buildings," *Journal of Engineering Mechanics*, ASCE 133:290-8
- Palermo M., Silvestri S. (2020). "Damping reduction factors for adjacent buildings connected by fluid-viscous dampers," *Soil Dynamics and Earthquake Engineering*, UK, 138:10632
- Nguyen D. V., Dookie K., Nguyen D. (2020). "Nonlinear seismic soil-structure interaction analysis of nuclear reactor building considering the effect of earthquake frequency content," *Structures*, NLD, 26:901-914.
- Djerouni S, Abdeddaim M, Ounis A (2021). "Seismic response control of adjacent buildings using optimal backward-shared tuned mass damper inerter and optimal backward-shared tuned inerter damper," *Asian Journal of Civil Engineering*, JPN, 22(8): 1499-1523.